# *Electrochemical sensing of 2D condensation in amyloid peptides*

Electrochimica Acta 106 (2013) 43–48

Contents lists available at SciVerse ScienceDirect

Electrochimica Acta

journal homepage: www.elsevier.com/locate/electacta

# Electrochemical sensing of 2D condensation in amyloid peptides

Katarzyna Kurzątkowska[a,c], Veronika Ostatná[a], Ian W. Hamley[d], Thomas Doneux[e], Emil Paleček[a,b,*]

[a] Institute of Biophysics ASCR, v.v.i., Kralovopolska 135, 612 65 Brno, Czech Republic
[b] Masaryk Memorial Cancer Institute, Zluty kopec 7, 656 53 Brno, Czech Republic
[c] Institute of Animal Reproduction and Food Research of Polish Academy of Sciences, Tuwima 10, 10-747 Olsztyn, Poland
[d] Department of Chemistry, University of Reading, Reading RG6 6AD, United Kingdom
[e] Chimie Analytique et Chimie des Interfaces, Faculté des Sciences, Université Libre de Bruxelles, Boulevard du Triomphe, 2, CP 255, B-1050 Bruxelles, Belgium

ARTICLE INFO

*Article history:*
Received 23 February 2013
Received in revised form 16 May 2013
Accepted 16 May 2013
Available online 23 May 2013

In memory of Professor Vladimir Vetterl.

*Keywords:*
Amyloid peptide sensing
2D condensed layers
Mercury–sulfur binding
Voltammetric and chronopotentiometric stripping
Catalytic hydrogen evolution

ABSTRACT

The interfacial behavior of the model amyloid peptide octamer YYKLVFFC (peptide **1**) and two other amyloid peptides YEVHHQKLVFF (peptide **2**) and KKLVFFA (peptide **3**) at the metal|aqueous solution interface was studied by voltammetric and constant current chronopotentiometric stripping (CPS). All three peptides are adsorbed in a wide potential range and exhibit different interfacial organizations depending on the electrode potential. At the least negative potentials, chemisorption of peptide **1** occurs through the formation of a metal—sulfur bond. This bond is broken close to −0.6 V. The peptide undergoes self-association at more negative potentials, leading to the formation of a "pit" characteristic of a 2D condensed film. Under the same conditions the other peptides do not produce such a pit. Formation of the 2D condensed layer in peptide **1** is supported by the time, potential and temperature dependences of the interfacial capacity and it is shown that presence of the 2D layer is reflected by the peptide CPS signals due to the catalytic hydrogen evolution. The ability of peptide **1** to form the potential-dependent 2D condensed layer has been reported neither for any other peptide nor for any protein molecule. This ability might be related to the well-known oligomerization and aggregation of Alzheimer amyloid peptides.



## 1. Introduction

Among human neurodegenerative diseases, special attention has been paid to diseases in which amyloidogenic proteins, when disturbed from their native state, can form oligomeric and polymeric aggregates [1,2]. Such aggregated proteins frequently have a well-defined fibrillar nature termed amyloid. A number of such diseases include type II diabetes, Creutzfeldt-Jakob, Alzheimer's and Parkinson's diseases. The latter two are the most common neurodegenerative disorders among the elderly. The amyloid β-peptides (Aβ) in Alzheimer's disease (AD) can serve as a paradigm for studies of amyloid formation and conformation [1,3]. These peptides derive from cleavage of the transmembrane amyloid precursor protein by secretases. Aggregation of AD and Parkinson's disease peptides and proteins can be induced or inhibited in vitro and in vivo by a number of agents. In vitro the aggregation was studied by different methods, such as circular dichroism, light scattering methods, polarized Raman spectroscopy, X-ray diffraction, thioflavin T or Congo red fluorescence, atomic force microscopy, electron microscopy or solid state NMR, etc. [1–4]. In recent years also electrochemical methods have been applied in such studies using carbon [5–7], Hg [4,6,8], and Au [9] electrodes. Interaction of Aβ peptides and proteins with lipid bilayers at Au and Hg [10,11] electrodes was also studied.

While most investigations have been carried out in solution, surface methods such as quartz crystal microbalance [3,12–16], surface plasmon resonance [17,18], microcantilever measurements [15,16,19], or electrochemical analysis [5–8,20] are increasingly being applied, allowing measurement of the growth of amyloid fibrils bound to a surface.

In the past decades electrochemistry of proteins concerned predominantly studies of non-protein components of conjugated proteins yielding reversible chemistry [21]. Oxidation of tyrosine (Tyr) and tryptophan residues in peptides [22] and proteins [23] at carbon electrodes was studied to a lesser extent. Recently it has been shown that using constant current chronopotentiometric stripping (CPS) practically all proteins and many peptides produce the so-called "peak H" (due to the catalytic hydrogen evolution reaction, CHER). This peak has proven to be valuable in protein structure analysis [24,25], and in studies of aggregation of amyloid protein α-synuclein [4,8].

In electrochemical techniques, reliable attachment of the peptide or protein to the surface plays a critical role. A recent strategy was proposed involving the reaction of cystamine and

* Corresponding author at: Institute of Biophysics ASCR, v.v.i., Kralovopolska 135, 612 65 Brno, Czech Republic. Tel.: +420 549 246 241; fax: +420 541 517 249.
*E-mail address:* palecek@ibp.cz (E. Paleček).

0013-4686 
http://dx.doi.org/10.1016/j.electacta.2013.05.057

2-iminothiolane with the amyloid fibrils, enabling their covalent linkage to gold surfaces via Au—S bonding [26]. Alternatively, cysteine-containing proteins can be attached to some metal surfaces, such as gold or mercury via Au-S or Hg—S bonds. This type of binding can however hardly be applied to AD Aβ-peptides or to α-synuclein (important in Parkinson's disease), lacking cysteine (Cys) residues. Non-covalent electrostatic binding of Aβ peptides to Au electrodes is much weaker and poorly suitable for the peptide immobilization at these electrodes. In Aβ-peptides, a Cys residue can be easily added to the given peptide during its synthesis. This was recently recognized by Partovi-Nia et al. [27] who modified the Aβ (12–28) peptide with a Cys residue at the C-terminal to immobilize it onto gold electrodes. With this platform, they were able to monitor electrochemically the interaction of the peptide with Congo Red and with a β-sheet breaker peptide.

We investigated the peptide-based octamer YYKLVFFC (peptide **1**) which contains the KLVFF Aβ (16–20) core domain with additional terminal Tyr and Cys residues to enable possible functionalization. This peptide was de novo designed by one of us (IWH). Cys residue enables not only covalent attachment to Hg and other metal surfaces but also chemical modification via the sulfhydryl moiety, and the two Tyr residues serve as fluorescence tags, and also potentially enable bioconjugation, or responsiveness to enzymes for instance via phosphorylation/dephosphorylation. The solution self-assembly of YYKLVFFC has been investigated using a variety of spectroscopic, scattering and microscopic methods [28]. The formation of β-sheet fibrils in peptide **1** was confirmed with a pH-dependent change in morphology. Remarkably, this peptide forms a nematic liquid crystal phase at relatively low concentration [28]. This tendency to spontaneously orient was later exploited in a detailed study of the orientation of the alignment of the peptide (in bulk solution, and dried films) using polarized Raman spectroscopy, linear UV dichroism, FTIR, X-ray diffraction and Near-Edge X-ray Absorption Fine Structure (NEXAFS) [29]. This provided detailed information on the orientation of fibrils and of the constituent Tyr fluorophores.

In the present work, we decided to supplement the wealth of information about properties of peptide **1** and other AD peptides obtained by the above methods by applying electrochemical methods, which proved useful in studies of oligomerization and aggregation of α-synuclein important in Parkinson's disease [4,6,8]. We focused on the electrochemical and interfacial properties of the above peptide **1** and two other Aβ peptides YEVHHQKLVFF (peptide **2**) and KKLVFFA (peptide **3**) predominantly at mercury electrodes. All three peptides contain the KLVFF core characteristic for the amyloid AD peptides. Peptide **3** differs from peptide **1** by changes at both termini. Two Tyr residues (YY) at the N-terminus of peptide **1** are replaced by K in peptide **3**, and C at the other end of peptide **1** is substituted by A in peptide **3**. In peptide **2** the KLVFF core is extended only at the N-terminus by YEVHHQ differing from both peptide **1** and **3** by negatively charged E, additional V and HH. The reduction of the Hg—S bond between the Hg surface and the Cys residue was evidenced only in peptide **1**. Besides the electroactive properties of the peptides, the interfacial behavior was investigated by differential capacity measurements. Peptide **1** (but not the other two peptides) showed a strong tendency to self-association and formation of 2D condensed layer at the electrode surface, which might be related to tendency of Alzheimer Aβ-peptides to aggregation.

## 2. Materials and methods

### 2.1. Reagents

The YYKLVFFC peptide was custom-synthesized by C.S. Bio Company (Menlo Park, CA) and was used as received as a TFA salt (purity > 96%). Details about the purity and characterization were published previously [29]. The KKLVFFA and YEVHHQKLVFF peptides were purchased from Bachem (Switzerland) (purity ≥95% respectively). Stock solutions were prepared by dissolving the peptides in triply distilled water and kept at 4 °C. The chemicals $Na_2HPO_4{\cdot}7\,H_2O$ (Sigma–Aldrich, >98.0%), $NaH_2PO_4{\cdot}H_2O$ (Sigma–Aldrich, >98.0%) and $Ru(NH_3)_6Cl_3$ (Sigma–Aldrich, >98.0%) were used as received.

### 2.2. Apparatus and electrochemical procedures

Electrochemical measurements were performed using an electrochemical 663 VA Stand multimode three-electrode systems (Metrohm, Herisau, Switzerland) connected with a μAutolab Analyzer type III or an Autolab electrochemical system PGSTAT 302 equipped with a frequency-response analyzer module (FRA2) (EcoChemie, Utrecht, The Netherlands). Hanging mercury drop electrode (HMDE, area of drop 0.4 $mm^2$) and basal plane pyrolytic graphite electrodes (PGE, 6.0 $mm^2$ area) were used as working electrodes, a Ag|AgCl|3M KCl electrode served as the reference electrode and a platinum wire as the auxiliary electrode. Cyclic voltammetry (CV), constant current chronopotentiometric stripping (CPS), differential pulse voltammetry (DPV) and alternating current (ac) voltammetry were employed in conjunction with an accumulation procedure. The chronopotentiometric and ac voltammetric experiments were performed under air. The CV and DPV measurements were done in the absence of oxygen, by passing argon through the solution for 10 min before the measurement, and above the solution during the measurement.

HMDE was held at the potential $E_A$ for an accumulation time $t_A$. In all experiments, stirring accompanied the accumulation. The CPS measurements were performed at an applied current of −11.0 μA, from an initial potential $E_i = -0.1$ V, if not stated otherwise. In ac voltammetry experiments, the potential perturbation had a frequency of 150 Hz and amplitude of 5.0 mV; the out-of-phase component was recorded at a scan rate of 8.0 mV $s^{-1}$, and converted to the differential capacity assuming a simple RC series circuit with a negligible resistance. The peptides were adsorbed for $t_A = 120$ s on PGE from a 20 μl drop of peptide solution, followed by washing of the peptide-modified electrode and its transfer to the electrolytic cell containing only the electrolyte (not containing any peptide).

## 3. Results and discussion

### 3.1. Electroactivity of peptides

The electrochemical activity of the YYKLVFFC (peptide **1**) and two additional Aβ-peptides not containing Cys was explored both at PGE and at HMDE, using different electrochemical methods. Combining these two electrode materials allows covering of a large potential window encompassing oxidation phenomena at very positive potentials (on carbon) and reduction ones at very negative potentials (on mercury). On the PGE, peaks due to Tyr were clearly evidenced by DPV for peptide **1** at +0.51 V (not shown) and for peptide **2** at +0.53 V while no oxidation peak appeared for peptide **3** not containing Tyr, in agreement with data earlier obtained with peptides [22] and proteins [23] and in studies of *a*-synuclein oligomerisation and aggregation [4,6,8] and of Aβ-peptide aggregation [5,7,20].

#### 3.1.1. Catalytic hydrogen evolution at mercury electrode

Peptide **1** produces two CPS peaks when adsorbed at HMDE at accumulation potential, $E_A$ −0.1 V (Fig. 1A). Peak, S centered around −0.65 V (Fig. 1A, inset) responds to the presence of Cys in this peptide and is assigned to the reduction of a Hg—S bond [30], indicating that the peptide is chemically immobilized at the electrode surface

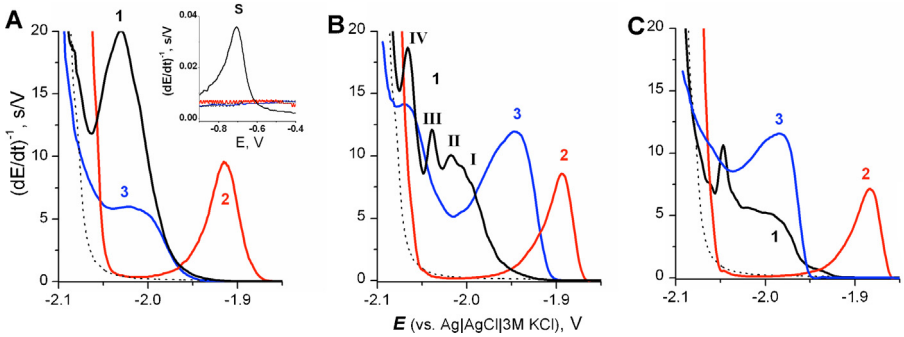


**Fig. 1.** CPS peaks H and S (inset) of YYKLVFFC (peptide **1**, black) YEVHHQKLVFF (peptide **2**, red) and KKLVFFA (peptide **3**, blue) at accumulation potential, $E_A$. (A) $E_A = -0.1$ V, (B) $E_A = -0.9$ V, (C) $E_A = -1.3$ V. Peaks were obtained in the presence of 2 μM peptides **1**–**3** in 35 mM phosphate buffer, pH 7.0 using HMDE at 25 °C; $t_A = 180$ s; $I_{str} = -11$ μA; background electrolyte (. . . . . ). (For interpretation of the references to color in the text, the reader is referred to the web version of the article.)

at potentials positive from the peak. Much higher peak H at very negative potentials is ascribed to CHER. In Fig. 1A a comparison of peaks H of the three peptides obtained under the same conditions is shown. Clearly, all three peptides produce specific peaks differing in their peak potentials, $E_p$ and/or in their heights. It has been shown that at neutral pH, accessible lysine (Lys, K), arginine (R) and Cys (C) residues in proteins are involved in CHER [31–33]. All three peptides studied in this paper contain K. Peptide **1**, which yielded the highest and most negative peak H at $E_A$ −0.1 V (Fig. 1A), contains (in addition to KK) one C. The heptameric peptide **3** produces a much smaller step-shaped signal shifted slightly to less negative potentials. Peptide **2** yielded the least negative symmetric peak H close to −1.9 V whose shape and height change only little in dependence on $E_A$ (see below). The above data are in agreement with our previous protein studies [24,34–38] showing great diversity in CPS responses of various peptides and proteins, suggesting that CPS may become useful in proteomics and biomedicine. Here we compared electrochemical behavior of the three Aβ-peptides to show the potential of electrochemical methods in amyloid peptide research. In our ac voltammetric studies we observed an unexpected property of peptide **1**, i.e. its ability to form a 2D condensed layer at the mercury electrode. To our knowledge such ability has been observed in nucleic bases [39–41] and oligonucleotides [42] but not in any peptides or proteins. The rest of this paper addresses therefore this phenomenon.

### 3.2. Peptide interfacial behavior

The adsorption of peptide **1** at the mercury|aqueous solution interface was studied by ac voltammetry, to obtain differential capacity–potential curves. Three adsorption regions can be distinguished (Fig. 2A), separated by two peaks centered at −0.58 V and −1.53 V. Like many peptides and other molecules bearing a thiol group, the Cys-containing peptide **1** can oxidatively form a Hg—S bond [30], and the pseudocapacitive peak at −0.58 V can be attributed to the reduction of this bond, as already evidenced above by CPS (cf. inset in Fig. 1A). At potentials positive of the peak (Region I), the peptide is thus chemisorbed at the interface through the formation of the Hg—S bond. In this region, the capacitance is rather insensitive to the potential indicating that the amount of adsorbed peptide does not vary significantly with the potential, as can be expected for a chemisorption phenomenon. By contrast, the capacitance was found to vary with the accumulation time, decreasing progressively with $t_A$ until reaching a constant value associated with the formation of a complete monolayer (Fig. 2B). At full coverage, the low value of the capacitance and its potential-independent character suggests the formation of a compact monolayer [43]. This is confirmed by its inhibiting properties toward the electron transfer of an electrochemically reversible redox marker, $[Ru(NH_3)_6]^{3+}$. Fig. 3 shows that at short accumulation times, the cyclic voltammograms recorded in the presence of $[Ru(NH_3)_6]^{3+}$ in solution have the usual characteristics associated with a reversible (fast kinetics) process. However, at larger values of $t_A$, the reduction wave is significantly shifted in the negative direction while the re-oxidation wave is slightly shifted in the positive direction, indicating a slow electron transfer attributed to the presence of the peptide monolayer at the surface.

While Peptide **1** exhibits a peak around −0.63 V and a roughly constant capacitance at less negative potentials (in agreement with presence of Cys in its molecule) (Fig. 2A), none of these features is noticeable for peptides **2** and **3** (Fig. 2A). On the contrary, in the latter peptides the capacitance is highly dependent on the potential and passes through a minimum, identified as the potential of maximum adsorption. Such a classical behavior is typical of the physisorption of a disordered layer [44,45]. At negative potentials the curve of peptide **2** is not below that obtained with blank background electrolyte (in absence of the peptide) suggesting that peptide **2** might be partially or fully desorbed from the surface. Fig. 2A shows that peptides **1** and **3** are still adsorbed on the electrode at potentials more negative than −0.65 V. All three peptides contain hydrophobic residues and basic Lys residues but the presence of glutamic acid (E) close to the —$NH_2$ terminus in peptide **2** can significantly affect the adsorption and orientation of the peptide molecule at the negatively charged surface [33]. It is therefore not surprising that under the given experimental conditions peptides **1** and **3** are still adsorbed at potentials as low as −1.7 V, as evidenced by the low capacitance recorded in this region (Region III) while peptide **2** shows a tendency to desorption already at potentials close to −1.0 V. In spite of this tendency peptide **2** produces CPS peak H (known to be produced by peptides and proteins in their adsorbed states) close to −1.9 V (Fig. 1). This could be due to the large difference between the rate of potential changes in ac voltammetry (scan rate 8 mV $s^{-1}$, Fig. 2A) as compared to CPS (~180 V/s at the given current density, Fig. 1). In CPS, the change in potential from −1.2 V to −1.9 V takes about 31 ms compared to >1 min in ac voltammetry. One can imagine that 31 ms may not be sufficient for complete desorption of a relatively large peptide molecule containing hydrophobic LVFF core in the close neighborhood of a positively charged Lys residue.

Of particular interest is the interfacial behavior of peptide **1**. The occurrence of three different regions of low capacitance indicates a potential-dependent adsorption behavior. Fig. 2B presents the capacity curves recorded for different accumulation times at the accumulation potential $E_A = -0.5$ V. It can be seen that for

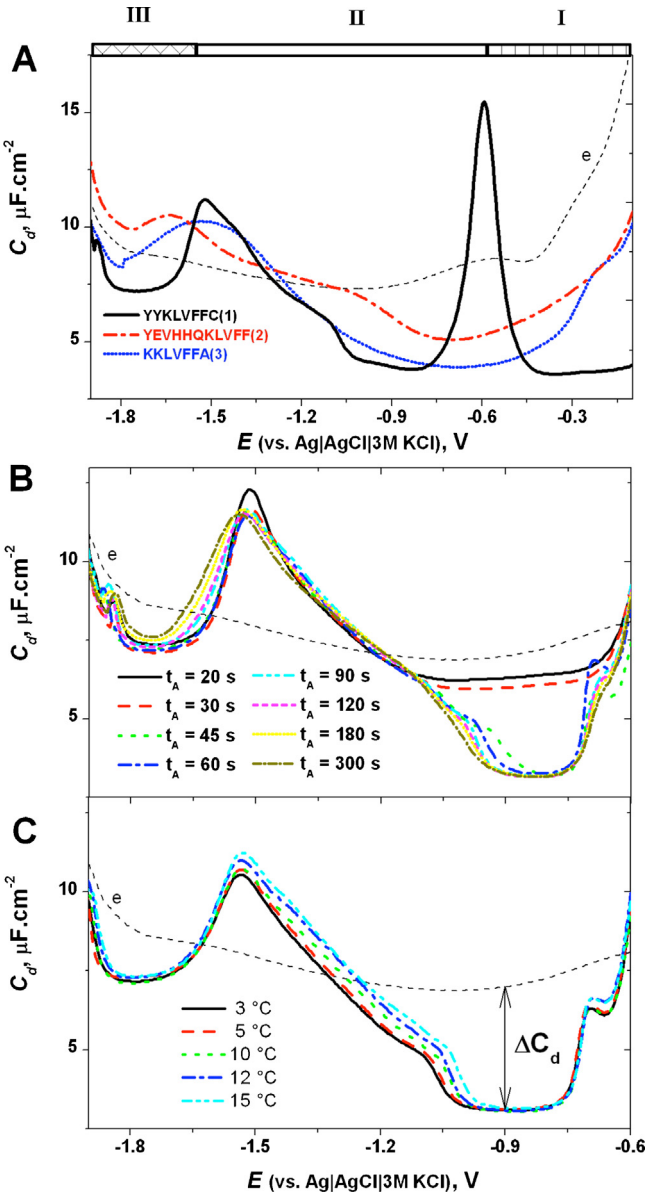


**Fig. 2.** (A) Capacity–potential curves of 1 µM peptide **1** (black), peptide **2** (red) and peptide **3** (blue) in 35 mM Na-phosphate, pH 7 (dashed line). Peptides were adsorbed at $E_A = -0.1$ V, for $t_A = 120$ s at HMDE, followed by recording of ac voltammogram with a frequency of 150 Hz and amplitude of 5.0 mV; scan rate of 8.0 mV s$^{-1}$. (B) Capacity–potential curves of 1 µM peptide **1** (YYKLVFFC) recorded in 35 mM phosphate buffer, pH 7.0 at 25 °C at different accumulation time $t_A$, as indicated on the graph. Accumulation potential $E_A = -0.5$ V. (C) Capacity–potential curves of 1 µM peptide **1** recorded in 35 mM phosphate buffer, pH 7.0 at different temperatures, as indicated on the graph. Accumulation potential $E_A = -0.5$ V; accumulation time $t_A = 120$ s. Other details are as in Fig. 1. (For interpretation of the references to color in the text, the reader is referred to the web version of the article.)

accumulation times up to 30 s, the capacitance is not much lower than for the bare electrode. At longer $t_A$, however, when larger quantities of peptide are adsorbed on the electrode, the capacitance suddenly drops to its minimum value, the curve forming a "capacitance pit" whose width progressively increases, in the negative direction, until reaching a constant value at times longer than 120 s (Fig. 2B). The capacitance value at the bottom of the pit expressed as $\Delta C$ (Fig. 2C) corresponds to 3.85 µF cm$^{-2}$. A larger width of the pit is indicative of a higher stability of the monolayer, provided by the attractive interactions between adsorbed molecules. The fact that the width significantly increases only in one direction is correlated with the chemisorption through the sulfur bond, which takes

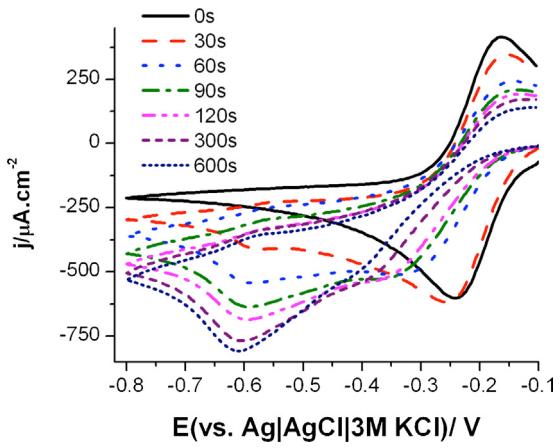


**Fig. 3.** Cyclic voltammograms recorded in 35 mM phosphate buffer pH 7.0 in the presence of 2.0 µM YYKLVFFC and 1 mM $[Ru(NH_3)_6]^{3+}$ after different accumulation times $t_A$, as indicated in the graph. Scan rate 100 mV s$^{-1}$; $E_A = -0.1$ V; HMDE.

place around the positive edge of the pit and is less sensitive to the amount of adsorbed peptide.

Our results show that it is not necessary to adsorb the peptide in the potential region where the Hg—S bond is formed (region I) to observe the pit. This was demonstrated by performing a set of experiments where the accumulation potential was located within the potential range of the pit, and the capacitance variation was monitored as a function of the accumulation time (not shown). Fig. 4 shows the capacity vs. time curves obtained at $E_A = -0.83$ V. In this set of experiments, a new drop was formed at the time $t_A = 0$ s, then the current was recorded while stirring the solution at a given rate. All the curves start from the same initial value corresponding to the capacitance of the bare electrode|electrolyte interface. A monotonic decrease of the capacitance is then observed, followed by a discontinuity in the form of a steep variation of the capacitance, then a final stabilization to a common value corresponding to the pit bottom. For every curve, the discontinuity occurs at a similar value of the capacitance or, conversely, a similar peptide coverage. Upon increasing the stirring rate, the initial decrease of the curves becomes faster, indicating a control by the mass transport of the peptide from the solution. However, if only mass transport were involved in the kinetics, the capacitance would continue to decrease in a monotonic fashion. By contrast, the shape of the curves demonstrates that another phenomenon takes place at a given threshold coverage. Such a shape is characteristic of systems undergoing 2D condensation [43,46], and is associated with the

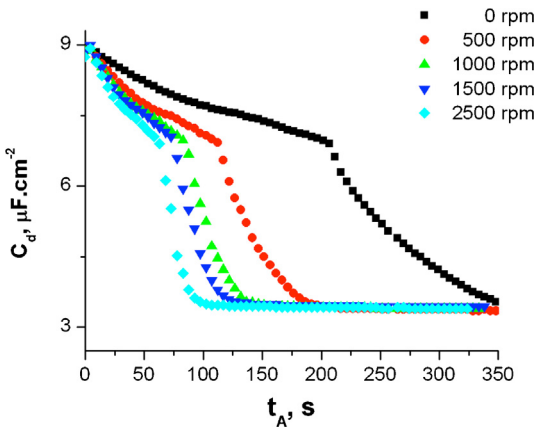


**Fig. 4.** Capacity vs. time transients recorded at $E_A = -0.83$ V in 35 mM phosphate buffer, pH 7.0 at 25 °C in the presence of 1 µM peptide **1** at different stirring rates, indicated on the graph. Other details are as in Fig. 2.

ordered phase formation kinetics. This experiment shows that the low capacitance recorded in region II corresponds to a real equilibrium state, and not to a possible metastable state. Fig. 2C shows that capacity of the pit bottom remains constant when varying the temperature. On the other hand the width of the pit increases with the temperature lowering. This behavior is typical of 2D condensed monolayers, confirming that a self-association process takes place in the potential range of the pit [47].

We were interested in whether the formation of the 2D layer will influence the CPS response of peptide **1**. We adsorbed peptide **1** at $E_A$ −0.9 V, i.e. within the pit, for $t_A$ 180 s, followed by recording of CPS peak H. Compared to peak H obtained after adsorbing this peptide at $E_A$ −0.1 V (Fig. 1A), the former adsorption resulted in four peaks H (I–IV) (Fig. 1B). Adsorption at $E_A$ −1.3 V negative to the pit resulted in a single peak close to $E_p$ of peak H-III obtained at $E_A$ −0.9 V (Fig. 1C). Similar experiments were performed with the two other peptides not forming any pit in their ac voltammograms (Fig. 2A). Adsorption of peptide **2** at the above $E_A$ values resulted in peaks H differing little in their heights but showing shifts in their $E_p$s to less negative values at more negative $E_A$s (Fig. 1). In contrast adsorption of peptide **3** at these three $E_A$s produced only a step-shaped signal at $E_A$ −0.1 V, while at $E_A$ −0.9 V and −1.3 V well developed peaks were obtained (Fig. 1). These results suggest that all three peptides can adsorb even at −1.3 V and during the fast potential changes in CPS, they still remain at the surface (probably attached by their hydrophobic parts) taking part in CHER close to −1.9 V (Fig. 1C), under conditions where their presence at the surface is not detectable by the slow scan capacitance measurement (Fig. 2A). No doubt, CPS peaks are highly sensitive to changes in the peptide layers adsorbed at the charged Hg surface. At this stage we are not able to explain the large number of CPS peaks obtained for peptide **1** after adsorption at $E_A$ −0.9 V. We can only speculate that during the fast potential changes in CPS from −0.9 V to about −2 V, the 2D layer is disturbed, yielding differently oriented peptide molecules at the surface, in which the CHER is more or less difficult, resulting in peaks at different potentials. More work will be necessary to understand better the relationship between the structure of the peptide 2D layer and its CPS responses.

Alignment of peptide **1** in bulk and at a solid silicon surface was studied by numerous methods [3,28,29]. Linear dichroism provided a picture of alignment of peptide strands and showed initial association of phenylalanine (F) residues followed by subsequent registry and orientation of Tyr residues. X-ray diffraction data from aligned stalks yielded orientation order parameters. Comparison of the results of polarized Raman spectroscopy with results from NEXAFS spectroscopy prepared as films on silicon indicated that fibril are aligned parallel to the surface with phenyl rings perpendicular to the surface. Formation of disulphide bridging was excluded by Raman spectroscopy and dityrosine formation probed by fluorescence experiments was found only at alkaline conditions but not at neutral pH. Peptide secondary structure was probed by Fourier-transform infrared (FTIR) and circular dichroism spectroscopies [28]. FTIR data showed features in the amide I region indicating antiparallel β-sheet structure. Taking the above results together we can conclude that they do not show any feature displaying striking difference between peptide **1** and other amyloid peptides and do not allow us at this stage to explain the unique ability of this peptide to form the 2D condensed layer. We can only speculate that it is the combination of the hydrophobic region (commonly present in amyloid peptides) with Cys —SH group (normally absent in amyloid peptides), and its strong affinity to mercury surfaces, which is involved in the 2D condensation of peptide **1**. On the other hand, our data (Fig. 2) and our previous experience [22,25,31] suggest that neither the hydrophobic region alone nor the —SH group alone was sufficient to induce formation of the peptide 2D layer.

## 4. Conclusions

We show that a model amyloid peptide **1** displays at the electrified interface electrochemical characteristics associated with the formation of a 2D condensed self-assembled monolayer (Fig. 2). Our results obtained with this peptide represent the first example of a potential-dependent 2D layer at an electrified interface in peptides and perhaps the second one among the biologically important oligomers. Earlier it was shown that interactions of hydrophobic bases with hydrophobic Hg electrodes play a critical role in DNA adsorption [48,49] at moderate ionic strengths. Similarly, it can be expected that hydrophobic residues in peptide **1** will be important in adsorption of this peptide at HMDE and might be involved in the ability to form a pit in the capacitance–potential curves. In peptides **2** and **3** the amyloid sequence KLVFF is identical with that of peptide **1** but peptide **2** does not show any sign of pit formation while peptide **3** displays only a small tendency to form a pit close to −0.2 V, greatly differing from the usual pits observed with peptide **1** (Fig. 2) or with DNA bases [40,41,50] and oligonucleotides [42]. Hydrophobic interactions play a critical role in Aβ-peptide oligomer and fibril formation [3]. Compared to in vitro solution experiments, studies on surfaces appear more biologically important because of its relevance to pathological processes occurring on various surfaces in cells and particularly in cell membranes. Some in vitro investigations indicated that presence of artificial or biological surfaces can greatly accelerate structural transition of Aβ peptides from random coil to β-sheet structure and to formation of heterogeneous Aβ-species [3]. Our finding of 2D condensed layer at negatively charged hydrophobic surface (Fig. 2) suggests that peptide **1** formed a densely packed ordered layer, which adhered strongly to the surface and removed small ions and water molecules from it. It is tempting to suggest that formation of this layer is related to the ability of peptide **1** to oligomerize and form larger aggregated species. We also demonstrate that peptide **1** can be covalently bound to HMDE thus providing a new way to immobilize Aβ-peptides to mercury surfaces (Fig. 1A, inset), suitable for studies on the growth of amyloid fibrils covalently attached to a surface. Moreover, we show for the first time that peak H can reflect formation of the condensed 2D layer (Fig. 1). Electrochemical methods and particularly the CPS peak H, which is highly sensitive to local changes in protein structures [36,51] can become very useful in Aβ peptide studies. Replacing HMDE by solid amalgam electrodes, which can easily be incorporated into peptide chips [52], may help to create a new tool for parallel analysis of Aβ peptides.

## Acknowledgements

This work was supported by a European Union Marie Curie Transfer of Knowledge Research Grant MTKD-CT-2006-042708. Th. D. gratefully acknowledges the financial support from Wallonie-Bruxelles International, EP from the GACR P301/11/2055 and by RECAMO CZ.1.05/2.1.00/03.0101. Research in the group of IWH was supported by EPSRC grants EP/G026203/1 and EP/G067538/1. We are indebted to Prof. V. Vetterl for his interest in our experiments and valuable advice and to Dr. V. Dorčák for critical reading of the manuscript.

## References

[1] Y. Miller, B. Ma, R. Nussinov, Polymorphism in Alzheimer Abeta amyloid organization reflects conformational selection in a rugged energy landscape, Chemical Reviews 110 (2010) 4820.
[2] I.W. Hamley, Peptide fibrillization, Angewandte Chemie International Edition 46 (2007) 8128.
[3] I.W. Hamley, The amyloid beta peptide: a chemist's perspective. Role in Alzheimer's and fibrillization, Chemical Reviews 112 (2012) 5147.
[4] C.D. Borsarelli, L.J. Falomir-Lockhart, V. Ostatna, J.A. Fauerbach, H.H. Hsiao, H. Urlaub, E. Palecek, E.A. Jares-Erijman, T.M. Jovin, Biophysical properties and

cellular toxicity of covalent crosslinked oligomers of alpha-synuclein formed by photoinduced side-chain tyrosyl radicals, Free Radical Biology & Medicine 53 (2012) 1004.
[5] J. Geng, H. Yu, J. Ren, X. Qu, Rapid label-free detection of metal-induced Alzheimer's amyloid β peptide aggregation by electrochemical method, Electrochemistry Communications 10 (2008) 1797.
[6] M. Masarik, A. Stobiecka, R. Kizek, F. Jelen, Z. Pechan, W. Hoyer, T.M. Jovin, V. Subramaniam, E. Palecek, Sensitive electrochemical detection of native and aggregated α-synuclein protein involved in Parkinson's disease, Electroanalysis 16 (2004) 1172.
[7] A.J. Veloso, K. Kerman, Modulation of fibril formation by a beta-sheet breaker peptide ligand: an electrochemical approach, Bioelectrochemistry 84 (2012) 49.
[8] E. Palecek, V. Ostatna, M. Masarik, C.W. Bertoncini, T.M. Jovin, Changes in interfacial properties of alpha-synuclein preceding its aggregation, Analyst 133 (2008) 76.
[9] I. Grabowska, H. Radecka, A. Burza, J. Radecki, M. Kaliszan, R. Kaliszan, Association constants of pyridine and piperidine alkaloids to amyloid beta peptide determined by electrochemical impedance spectroscopy, Current Alzheimer Research 7 (2010) 165.
[10] E. Protopapa, L. Ringstad, A. Aggeli, A. Nelson, Interaction of self-assembling beta-sheet peptides with phospholipid monolayers: the effect of serine, threonine, glutamine and asparagine amino acid side chains, Electrochimica Acta 55 (2010) 3368.
[11] E. Protopapa, S. Maude, A. Aggeli, A. Nelson, Interaction of self-assembling beta-sheet peptides with phospholipid monolayers: the role of aggregation state, polarity, charge and applied field, Langmuir 25 (2009) 3289.
[12] H. Okuno, K. Mori, T. Okada, Y. Yokoyama, H. Suzuki, Development of aggregation inhibitors for amyloid-beta peptides and their evaluation by quartz-crystal microbalance, Chemical Biology & Drug Design 69 (2007) 356.
[13] H. Ogi, Y. Fukunishi, T. Yanagida, H. Yagi, Y. Goto, M. Fukushima, K. Uesugi, M. Hirao, Dependent deposition behavior of Aβ peptides studied with wireless quartz-crystal-microbalance biosensor, Analytical Chemistry 83 (2011) 4982.
[14] A.K. Buell, G.G. Tartaglia, N.R. Birkett, C.A. Waudby, M. Vendruscolo, X. Salvatella, M.E. Welland, C.M. Dobson, T.P.J. Knowles, Position-dependent electrostatic protection against protein aggregation, ChemBioChem 10 (2009) 1309.
[15] J.A. Kotarek, K.C. Johnson, M.A. Moss, Quartz crystal microbalance analysis of growth kinetics for aggregation intermediates of the amyloid-beta protein, Analytical Biochemistry 378 (2008) 15.
[16] D.A. White, A.K. Buell, C.M. Dobson, M.E. Welland, T.P.J. Knowles, Biosensor-based label-free assays of amyloid growth, FEBS Letters 583 (2009) 2587.
[17] J. Ryu, H.-A. Joung, M.-G. Kim, C.B. Park, Surface plasmon resonance analysis of Alzheimer's β-amyloid aggregation on a solid surface: from monomers to fully-grown fibrils, Analytical Chemistry 80 (2008) 2400.
[18] W.P. Hu, G.L. Chang, S.J. Chen, Y.M. Kuo, Kinetic analysis of beta-amyloid peptide aggregation induced by metal ions based on surface plasmon resonance biosensing, Journal of Neuroscience Methods 154 (2006) 190.
[19] M.J. McMasters, R.P. Hammer, R.L. McCarley, Surface-induced aggregation of beta amyloid peptide by omega-substituted alkanethiol monolayers supported on gold, Langmuir 21 (2005) 4464.
[20] M. Vestergaard, K. Kerman, M. Saito, N. Nagatani, Y. Takamura, E. Tamiya, A rapid label-free electrochemical detection and kinetic study of Alzheimer's amyloid beta aggregation, Journal of the American Chemical Society 127 (2005) 11892.
[21] H. Wackerbarth, J. Zhang, M. Grubb, H. Glargaard, B.L. Ooi, H.E.M. Christensen, J. Ulstrup, Self-assembly of biomolecules on electrode surfaces;oligonucleotides, amino acid, and proteins towards the single-molecule level, in: E. Palecek, F. Scheller, J. Wang (Eds.), Electrochemistry of Nucleic Acids and Proteins. Towards Electrochemical Sensors for Genomics and Proteomics, Elsevier, Amsterdam, 2005, p. 485.
[22] X.H. Cai, G. Rivas, P.A.M. Farias, H. Shiraishi, J. Wang, E. Palecek, Potentiometric stripping analysis of bioactive peptides at carbon electrodes down to subnanomolar concentrations, Analytica Chimica Acta 332 (1996) 49.
[23] V. Ostatna, H. Cernocka, K. Kurzatkowska, E. Palecek, Native and denatured forms of proteins can be discriminated at edge plane carbon electrodes, Analytica Chimica Acta 735 (2012) 31.
[24] V. Ostatna, E. Palecek, Native, denatured and reduced BSA – enhancement of chronopotentiometric peak H by guanidinium chloride, Electrochimica Acta 53 (2008) 4014.
[25] E. Palecek, V. Ostatna, Electroactivity of nonconjugated proteins and peptides. Towards electroanalysis of all proteins, Electroanalysis 19 (2007) 2383.
[26] A.K. Buell, D.A. White, C. Meier, M.E. Welland, T.P.J. Knowles, C.M. Dobson, Surface attachment of protein fibrils via covalent modification strategies, Journal of Physical Chemistry B 114 (2010) 10925.
[27] R. Partovi-Nia, S. Beheshti, Z. Qin, H.S. Mandal, Y.-T. Long, H.H. Girault, H.-B. Kraatz, Study of amyloid β-peptide (Aβ12-28-Cys) interactions with congo red and β-sheet breaker peptides using electrochemical impedance spectroscopy, Langmuir 28 (2012) 6377.
[28] I.W. Hamley, V. Castelletto, C. Moulton, D. Myatt, G. Siligardi, C.L.P. Oliveira, J.S. Pedersen, I. Abutbul, D. Danino, Self-assembly of a modified amyloid peptide fragment: pH-responsiveness and nematic phase formation, Macromolecular Bioscience 10 (2010) 40.
[29] I.W. Hamley, V. Castelletto, C.M. Moulton, J. Rodriguez-Perez, A.M. Squires, T. Eralp, G. Held, M.R. Hicks, A. Rodger, Alignment of a model amyloid peptide fragment in bulk and at a solid surface, Journal of Physical Chemistry B 114 (2010) 8244.
[30] M. Heyrovsky, P. Mader, S. Vavricka, V. Vesela, M. Fedurco, The anodic reactions at mercury electrodes due to cysteine, Journal of Electroanalytical Chemistry 430 (1997) 103.
[31] T. Doneux, V. Dorcak, E. Palecek, Influence of the interfacial peptide organization on the catalysis of hydrogen evolution, Langmuir 26 (2010) 1347.
[32] M. Zivanovic, M. Aleksic, V. Ostatna, T. Doneux, E. Palecek, Polylysine-catalyzed hydrogen evolution at mercury electrodes, Electroanalysis 22 (2010) 2064.
[33] V. Dorcak, V. Ostatna, E. Palecek, Electrochemical reduction and oxidation signals of angiotensin peptides. Role of individual amino acid residues, Electrochemistry Communications 31 (2013) 80.
[34] E. Palecek, M. Bartosik, V. Ostatna, M. Trefulka, Electrocatalysis in proteins, nucleic acids and carbohydrates, The Chemical Record 12 (2012) 27.
[35] E. Palecek, V. Ostatna, Ionic strength-dependent structural transition of proteins at electrode surfaces, Chemical Communications (2009) 1685.
[36] V. Ostatna, H. Cernocka, E. Palecek, Protein structure-sensitive electrocatalysis at dithiothreitol-modified electrodes, Journal of the American Chemical Society 132 (2010) 9408.
[37] E. Palecek, V. Ostatna, H. Cernocka, A.C. Joerger, A.R. Fersht, Electrocatalytic monitoring of metal binding and mutation-induced conformational changes in p53 at picomole level, Journal of the American Chemical Society 133 (2011) 7190.
[38] V. Dorcak, E. Palecek, Electrochemical determination of thioredoxin redox states, Analytical Chemistry 81 (2009) 1543.
[39] V. Vetterl, Adsorption of dna components on mercury electrode, Experientia 21 (1965) 9.
[40] V. Vetterl, S. Hason, Electrochemical properties of nucleic acid components, in: E. Palecek, F. Scheller, J. Wang (Eds.), Electrochemistry of Nucleic Acids and Proteins, 1, Elsevier, Amsterdam, 2005, p. 17.
[41] S. Hason, V. Vetterl, Two dimensional condensation of nucleic acid components at mercury film and gold electrodes, Bioelectrochemistry 56 (2002) 43.
[42] S. Hason, V. Vetterl, M. Fojta, Two-dimensional condensation of pyrimidine oligonucleotides during their self-assemblies at mercury based surfaces, Electrochimica Acta 53 (2008) 2818.
[43] C. Buess-Herman, Self-assembled monolayers at electrode metal surfaces, Progress in Surface Science 46 (1994) 335.
[44] B.B. Damaskin, V.E. Kazarinov, The adsorption of organic molecules, in: J.O.M. Bockris, B.E. Conway, E. Yeager (Eds.), Comprehensive Treatise of Electrochemistry, 1, Plenum Press, New York, 1980, p. 353.
[45] A.N. Frumkin, B.B. Damaskin, Adsorption of organic compounds at electrodes, in: J.O.M. Bockris, B.E. Conway (Eds.), Modern Aspects of Electrochemistry, 3, Butterworths, London, 1964, p. 149.
[46] R. De Levie, The dynamic double layer: two-dimensional condensation at the mercury-water interface, Chemical Reviews 88 (1988) 599.
[47] U. Retter, V. Vetterl, J. Jursa, On the stability of condensed adsorption films, Journal of Electroanalytical Chemistry 274 (1989) 1.
[48] E. Palecek, M. Bartosik, Electrochemistry of nucleic acids, Chemical Reviews 112 (2012) 3427.
[49] V. Ostatna, E. Palecek, Self-assembled monolayers of thiol-end-labeled DNA at mercury electrodes, Langmuir 22 (2006) 6481.
[50] V. Vetterl, Adsorption of nucleosides on mercury surface, Biophysik 5 (1968) 255.
[51] V. Ostatna, H. Cernocka, E. Palecek, Simple protein structure-sensitive chronopotentiometric analysis with DTT-modified Hg electrodes, Bioelectrochemistry 87 (2012) 84.
[52] P. Juskova, V. Ostatna, E. Palecek, F. Foret, Fabrication and characterization of solid amalgam electrodes array for bioanalytical applications, Analytical Chemistry 82 (2010) 2690.